Growth and characterization of epitaxial bismuth films

D. L. Partin, J. Heremans, D. T. Morelli, C. M. Thrush, C. H. Olk, and T. A. Perry
Physics Department, General Motors Research Laboratories, Warren, Michigan 48090
(Received 7 March 1988)

The present work describes the growth of the first thin (0.1–2 μm) epitaxial films of pure bismuth using molecular-beam-epitaxy techniques. These structures were grown at elevated temperatures on single-crystal barium fluoride substrates of ⟨111⟩ orientation. Electron-microscope observations show the films to be featureless and defect free on the scale of 0.1 μm. The films grow with their trigonal axis parallel to the ⟨111⟩ axis of the substrate, and Laue-backscattering pictures show they are epitaxial. Mobilities at room temperature are on the order of 2 $m^2 V^{-1} s^{-1}$, and increase to over 10 at 20 K and 100 at liquid-helium temperatures. These values are far superior to those of other bismuth films grown to date, and approach mobilities observed in single-crystal bismuth. Further evidence of their single-crystal nature is given by the temperature-dependent resistivity below 6K, which is more akin to that of a bulk single crystal, rather than polycrystal, bismuth, and by the thickness dependence of the film mobilities, which are limited by scattering on film boundaries. The carrier density, as deduced from Hall measurements, is in the range $(4-8)\times 10^{24}$ m^{-3} at room temperature and decreases as the temperature is lowered, becoming constant below about 50 K at approximately 5×10^{23} m^{-3}. We also observe Shubnikov–de Haas oscillations in the resistivity and Hall coefficient at 4.2 and 0.4 K. The carrier density calculated from the period of these oscillations correlates well with that found from Hall measurements.

INTRODUCTION

Bismuth is the solid in which the first manifestations of quantum size effects may have been observed, in films[1,2] or in wires.[3] Size-quantization effects are expected to be very pronounced in Bi films because the electron effective mass is very small and structures can potentially be made which have dimensions considerably smaller than the electron deBroglie wavelength. If Bi films were made thin enough (<10 nm), size quantization of the electron and hole bands should drive the energy levels high enough that the band overlap present in the bulk solid is transformed into a band gap:[4] Takaoka and Murase[5] may have observed this using optical techniques on preferentially aligned polycrystalline films that were grown on ⟨111⟩ BaF_2. Finally a new band-inverted semiconductor junction involving $Bi/Bi_{1-x}Sb_x$ heterojunctions has been proposed[6] that may contain subbands of a new type[7] in its gap. The growth of epitaxial Bi films is the first necessary step in investigating such structures.

The growth and properties of bismuth thin films have been the subject of some experimentation over the years. Garcia, Kao, and Strongin[2] grew bismuth on mica and found an average crystallite size of 1 μm. The resistivity of their films was significantly higher than that of bulk bismuth, and the magnetoresistance was substantially diminished. Many other, even recent, investigations[8–11] produced films whose resistivity was not even metallic in nature. Compositionally modulated superlattices of Bi and PbTe (Ref. 12) and of Bi and Sb (Ref. 13) were also grown, but had similar problems: Typically the trigonal axis of Bi would align perpendicularly to the substrate, but the in-plane structure of the film would be polycrystalline, or at least twinned. All of these films possessed greatly diminished mobilities due to poor crystallinity of the film.

In this paper we describe the growth and galvanomagnetic properties of the first (to our knowledge) truly epitaxial Bi films, which have mobilities comparable to those of bulk Bi, and show Shubnikov–de Haas oscillations.

EXPERIMENTAL TECHNIQUES

We have grown our bismuth films using a Physical Electronics model 400 molecular-beam-epitaxy (MBE) apparatus. This equipment has been previously described.[14] In brief, the MBE system is load-locked and also has an ion-pumped preparation chamber with a base pressure of 10^{-9} Torr in which the samples may be heated before growth. Finally, the samples are transferred to a cryopumped growth chamber with a base pressure of 10^{-10} Torr. The growth chamber was equipped with a reflection high-energy electron-diffraction (RHEED) system, but this was generally not useful for observing the initial stages of nucleation and growth, since the BaF_2 substrates used were severely damaged (roughened) by brief electron-beam exposure. The pressure during growth was usually in the mid-10^{-10}-Torr range and the growth rate was 0.5 μm/h.

As a substrate for the growth of bismuth we have chosen freshly cleaved single-crystal barium fluoride. Its ⟨111⟩-oriented cleavage plane has a crystal lattice constant of 6.200 Å at room temperature, which is relatively close (3.6%) to that of bismuth in its trigonal orientation (6.429 Å). The substrate holder is provided with a heater and a thermocouple to allow for growth at different substrate temperatures after nucleation at reduced temperature.

Two sets of film series were grown: (a) a series of films 500 nm thick which were grown at temperatures of 20, 240, 250, and 260 °C (the melting point of bismuth is 271 °C, and (b) a series of films grown at 250 °C and with thicknesses of 100, 150, 250, 500, 1000, and 2000 nm. The designation of these samples is given in Table I.

Preliminary transmission electron diffraction patterns taken on our Bi films[15] indicate that Bi grows with its trigonal ⟨001⟩ axis oriented parallel with the substrate ⟨111⟩ axis, as it usually does on BaF_2,[5] mica,[2] or PbTe.[12] Laue-backscattering pictures taken along that ⟨001⟩ axis on the 2-μm-thick film (sample no. 11) grown at 250 °C have threefold symmetry, indicating that it is truly epitaxial.

The galvanomagnetic properties of the films were measured as a function of temperature (0.4 to 350 K) in three different cryostats. The field was oriented perpendicularly to the film plane, i.e., parallel to the trigonal direction. Because of the crystal symmetry, the resistivity and Hall components are isotropic in the film plane. We thus measure the magnetoresistance tensor components $\rho_{11}(B_3)$ and $\rho_{12}(B_3)$. Because of the presence of cleavage steps in the underlying barium fluoride substrate, it was necessary to confine the measurements to an area of the film free of such defects. Such regions were identified by observing the sample under a high-power microscope. In order to provide a well-defined sample size the sample was etched into a six-point bridge pattern, which allowed for current contacts as well as both resistive and Hall-voltage contacts. The active channel of the sample was 40 μm wide and 200 μm in length. An etch consisting of 1:1:1 H_2O, HCl, and HNO_3 was used to define the sample shape employing standard photolithographic techniques. Electrical contact to the sample was made with small drops of conductive silver paint. The sample thus prepared was glued to the cold tip of the cryostat, and measurement of the Hall voltage and resistance as a function of field perpendicular to the film surface were made at a series of fixed temperatures.

All samples were measured in a closed-cycle refrigerator at temperatures ranging from 20 to 350 K and fields from 0 to 2 T. A series of samples grown at 250 °C, of thickness varying between 10 and 200 nm (sample nos. 11, 12, 4, 10, and 8) were measured immersed in liquid He at 4.2 K, in fields up to 17 T. Shubnikov–de Haas oscillations become clearly visible in resistance and Hall voltage. In addition to the above measurements, two samples, nos. 2 and 5, were inserted in a ^{3}He cryostat capable of reaching 0.3 K and fitted with a 7-T superconducting solenoid. This allowed for the determination of the resistivity as a function of temperature at very low temperatures. For all galvanomagnetic measurements, both the field and the current were reversed in order to eliminate errors due to probe misalignment and thermal offsets.

TABLE I. Sample parameters.

Designation	Growth temperature (°C)	Thickness (nm)
1	20	528
2	240	515
3	240	529
4	250	500
5	260	500
6	250	100
7,8	250	150
9,10	250	250
11	250	2000
12	250	1000

RESULTS AND DISCUSSION

Structure

The surface morphology of the films was investigated using a scanning-electron microscope. Figure 1(a) shows an image of sample 1, a 500-nm-thick film grown at 20 °C. Noticeable features in the surface morphology of this film can be seen. Specifically, the mottled appearance of the surface is apparently due to randomly oriented crystallites of approximate dimensions of 1 μm. Evidently the

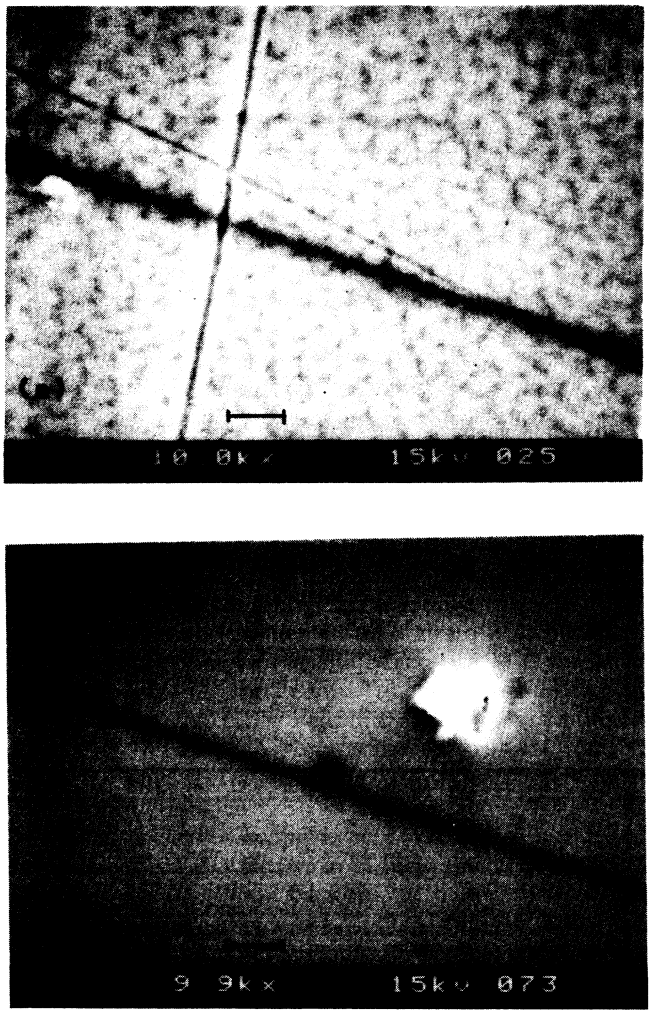

FIG. 1. Scanning-electron micrographs of two bismuth thin films: (a) sample 1, grown at 20 °C; (b) sample 3, grown at 240 °C. Scale is 1 μm.

films grow by island formation, and at this growth temperature grain boundaries form between the islands as they coalesce and are not annealed out of the structure. Also visible in this micrograph are two crossed straight lines. These replicate cleavage steps in the underlying barium fluoride substrate. In Fig. 1(b) we display a micrograph of a second sample, no. 3, which was grown at 240 °C and is also 500 nm thick. We see that in this case there are no observable features on the bismuth surface, aside from a small chunk of insulating material which is most likely a particle of barium fluoride left on the surface after cleavage. Thus it appears that growth at an elevated temperature allows sufficient movement of the bismuth atoms on the substrate surface to produce an ordered, nearly perfectly crystalline surface.

Galvanomagnetic properties

Because the mobility of the films investigated here is so high, the low-field limit of the Boltzmann equations is violated even by a field of a few tenths of a tesla. Since bismuth is a semimetal with a small band overlap, both electrons and holes participate in the conduction process, and in order to determine the electron and hole mobilities and densities, a complete two-carrier, intermediate-field model must be used. Furthermore, the anisotropic nature of the Fermi surfaces of both charge carriers imposes the use of anisotropic mobility tensors.[16] In order to limit the number of adjustable parameters, we assumed that the relaxation time is isotropic, though different for electrons and holes. The resulting carrier mobilities in the different directions then scale as the inverse of the effective masses. This hypothesis is supported by the data available for the mobilities of bulk samples.[16] The holes fill two half-ellipsoidal Fermi surfaces at the T points of the Brillouin zone.[17] These ellipsoids have circular symmetry around the $\langle 001 \rangle$ axis. The electrons fill six half-ellipsoids at the L points, with the principal axes located as follows: The shortest axis of the ellipsoids is parallel to the binary $\langle 100 \rangle$ axis; the longest ellipsoid principal axis is in the bisectrix-trigonal plane, tilted by an angle $\phi = 7°$ with respect to the bisectrix $\langle 010 \rangle$ axis. As adjustable parameters we used the electron and hole densities (n and p, respectively), the in-plane hole mobility ν (isotropic in the film plane), and the electron mobility μ along $\langle 100 \rangle$ for the one L-point ellipsoid whose shortest principle axis aligns with the chosen $\langle 100 \rangle$ axis. The two other electron ellipsoids then have their shortest principal axis 120° off that $\langle 100 \rangle$ direction, and since $\mu_{\langle 010 \rangle} \ll \mu_{\langle 100 \rangle}$, the average in-plane mobility of all electrons is about 0.5μ. At each experimental temperature we measured the magnetoresistance and Hall effect at seven values of the field ranging from 0 to 2 T, and the magnetoresistivity data were inverted into magnetoconductivity data. A computer fit to the latter then yielded n, p, μ, and ν.

Figure 2 shows the electron and hole densities and mobilities for five samples, representative of the two series: (a) three samples (nos. 1, 4, and 5) each 500 nm thick, grown at 20, 250, and 260 °C, respectively; (b) three samples (Nos. 11, 4, and 6) each grown at 250 °C, and 2000, 500, and 100 nm thick, respectively. For comparison we also show the densities and mobilities of bulk single-crystal bismuth.[16]

The effect of film thickness and growth temperature on the carrier densities is displayed in Figs. 2(a) and 2(b). It must be pointed out that the apparent saturation of the hole density [Fig. 2(b)] at temperatures above 270 K is not significant: The holes contribute less than 30% to the electrical conduction and the values of their density obtained through galvanomagnetic data fitting is not accurate to better than ±20% in that temperature range. This problem was avoided in Ref. 16 by postulating that $n = p$. Since we were concerned with possible carrier-density enhancements in these epitaxial films, we fitted n and p separately. In retrospect, we can conclude that the electron and hole densities are indeed equal. Similar to bulk bismuth, the carrier density below 50 K is independent of temperature, but as the temperature is raised above this value, the carrier density increases. This is in accord with the model of Lopez,[18] which shows that carrier generation from the valence to the conduction band occurs for phonon energies greater than 43 K. We see that the carrier density is fairly insensitive to growth temperature. This indicates that whereas the scattering mechanisms are significantly affected by the film morphology, the electronic structure remains, for the most part, unchanged. The dependence of density on film thickness will be discussed in a later paragraph.

Figures 2(c) and 2(d) shows the temperature dependence of electron and hole mobilities. Room-temperature mobilities in the films are on the order of 2 $m^2 V^{-1} s^{-1}$, about a factor of 1.5 lower than the bulk, but the T^{-2} dependence is very similar to that of single crystals (and vastly different from the nearly-temperature-independent mobility observed in bismuth films grown on sapphire[19]), indicating that significant inelastic (i.e., carrier-phonon or perhaps interpocket carrier-carrier) scattering occurs down to at least 100 K. Below this temperature the mobilities begin to saturate, with a saturation value dependent on the growth temperature and film thickness. Figure 3, in fact, shows the mobilities at 20 K versus growth temperature, and we see indeed that the mobility in the samples grown at higher temperature is significantly larger. This merely reflects the changes which occur in the film morphology under varying growth conditions, as discussed above.

In Fig. 4 we plot the carrier densities (triangles, right-hand ordinate) and mobilities (circles, left-hand ordinate) versus film thickness for films grown at 250 °C. Thicker films have higher mobility, which suggests that the mean free path of the carriers is limited by the film boundaries. For films thinner than 250 nm, the mobility-thickness curves do not extrapolate to the origin (dashed line), but rather cross the abscissa at 20–50 nm. That could point to the existence of a "dead" layer of about that thickness which would have poor crystal quality. Our attempts to grow 20-nm-thick Bi layers gave films that were electrically continuous, but the galvanomagnetic data at 18 K can only be fitted to carrier densities an order of magnitude larger than the other films, and to mobilities of about 0.3 $m^2 V^{-1} s^{-1}$. The increase in density and de-

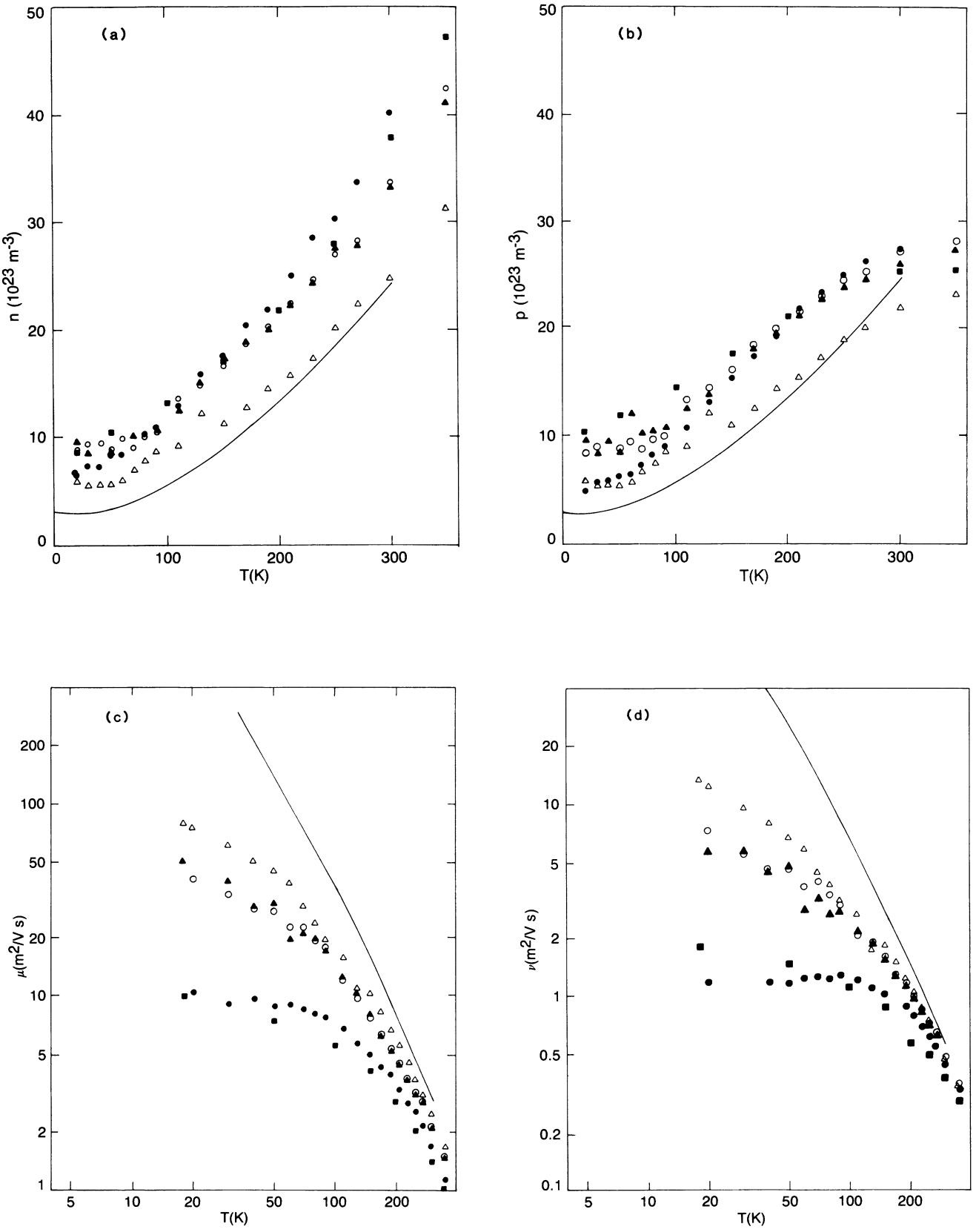

FIG. 2. Temperature dependence of the (a) electron and (b) hole densities and (c) electron and (d) hole mobilities in bismuth thin films. Sample designation: ●—1, ○—4, ▲—5 (500 nm thick, growth temperatures of 20, 240, and 260 °C, respectively); ■—6, ○—4, △—11 (grown at 250 °C, 100, 500, and 2000 nm thick, respectively). Solid lines indicate bulk properties.

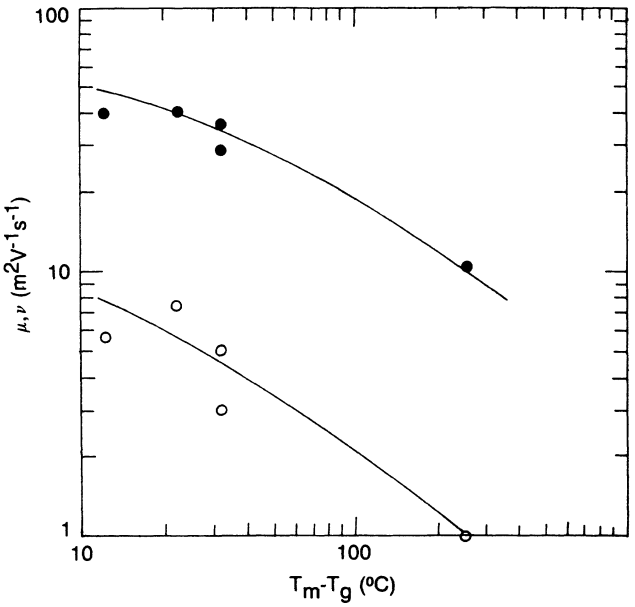

FIG. 3. Mobilities of electrons (●) and holes (○) at 20 K as a function of the growth temperature T_g. $T_m = 271$ °C is the melting point of bismuth.

crease in mobility in the "dead" layer is the possible cause for the apparent increase in density as the film thickness is decreased, as seen in Fig. 4. Since size-quantization effects invalidate the model used in the fit, and since 20-nm-thick films may be air sensitive, further work is needed to grow and characterize very thin epitaxial Bi layers.

Results of our high-precision electrical-resistivity studies on sample 2 are shown in Fig. 5. According to Matthiessen's rule the resistivity can be written

$$\rho = \rho_0 + \rho_t \ ,$$

where ρ_0 is a temperature-independent resistivity due to impurity, defect, and boundary scattering, and ρ_t is the resistivity due to intrinsic (such as electron-phonon) processes. The inset of Fig. 5 shows $\rho - \rho_0$ as a function of temperature between 1 and 6 K. Also shown are published results for the temperature-dependent resistivity of bulk single-crystal and polycrystal bismuth.[20] We see that our sample has an intrinsic resistivity identical to that of single-crystal bismuth, further attesting to the epitaxial quality of our films.

We have also observed what we believe to be the first quantum oscillations on a bismuth film. These are shown in Fig. 6, where we plot the magnetoresistance ρ_{xx} and the Hall resistivity ρ_{xy} of our films at 4.2 K as a function of the applied magnetic field up to 17 T. Shubnikov–de Haas oscillations are clearly seen in both galvanomagnetic coefficients. The amplitude of the quantum oscillations is larger in ρ_{xy} than in ρ_{xx} because the monotonic electron and hole contributions tend to cancel each other in the Hall component, while they add up in the magnetoresistance. The inset in Fig. 6(b) shows the Hall voltage at lower fields in which we find a period of $(8.0\pm0.3)T^{-1}$. If this period is ascribed to holes, then, in the free-electron approximation,[21]

$$\Delta(1/B) = E_F m_c/\hbar e \ ,$$

where E_F is the hole Fermi energy and m_c the cyclotron mass. Using the value $m_c = 0.064 m_0$,[22] we find from the measured period a hole Fermi energy of approximately

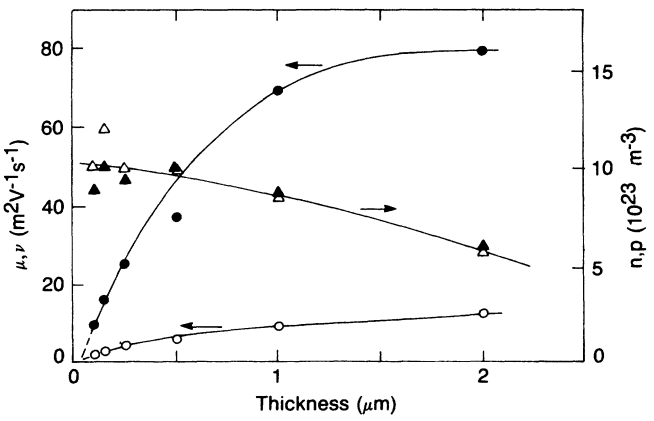

FIG. 4. Carrier mobilities and densities at 20 K as a function of layer thickness for films grown at 250 °C. ○—hole mobility, ●—electron mobility, △—hole density, ▲—electron density.

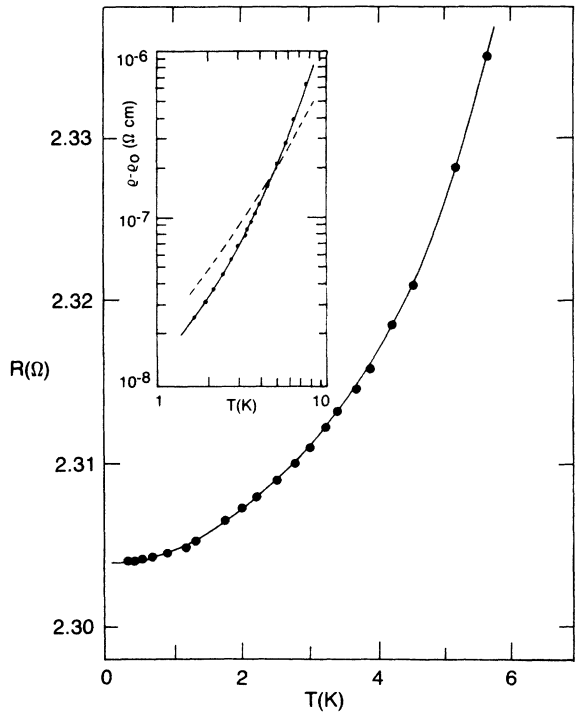

FIG. 5. Electrical resistivity of sample 2 at very low temperatures. Inset shows temperature-dependent part as well as results for bulk single crystal (solid line) and polycrystal (dashed line).

14.5 meV. This corresponds to a hole density of approximately 4.2×10^{23} m^{-3}. Using on these data the same two-carrier intermediate-field fitting routine that we used to interpret the high-temperature data, we obtain $n\sim p\simeq(5\pm1)\times10^{23}$ m^{-3}, in good agreement with the Shubnikov–de Haas period. The corresponding electron and hole mobilities are $\mu\simeq80$ $m^2V^{-1}s^{-1}$ and $\nu\simeq3$ $m^2V^{-1}s^{-1}$. At higher magnetic fields, the oscillations no longer are periodic in $1/B$, because the carrier density changes,[23] becoming, in fact, a linear function of field when the electrons are all on the lowest Landau level. A calculation of this density dependence on the magnetic field applied in the trigonal direction was made in Ref. 23, and dividing the magnetostrictive strain shown in Fig. 4 of that paper by 3.2×10^{-23} cm^3 yields the density in a straightforward manner for bulk bismuth. In films 250 and 150 nm thick, ρ_{xx} and ρ_{xy} still show oscillations, but assigning them is not as straightforward as in the thicker films. One must assume that size quantization does influence the Fermi surfaces, particularly of the electrons because their mass in the [001] direction is only $0.0023m_0$.[22] A quantitative model for the size-quantized fan chart of the bismuth energy levels can be developed, but the presence of the "dead" layer in these samples may make a full quantitative analysis of the data on films less than 250 nm thick somewhat futile.

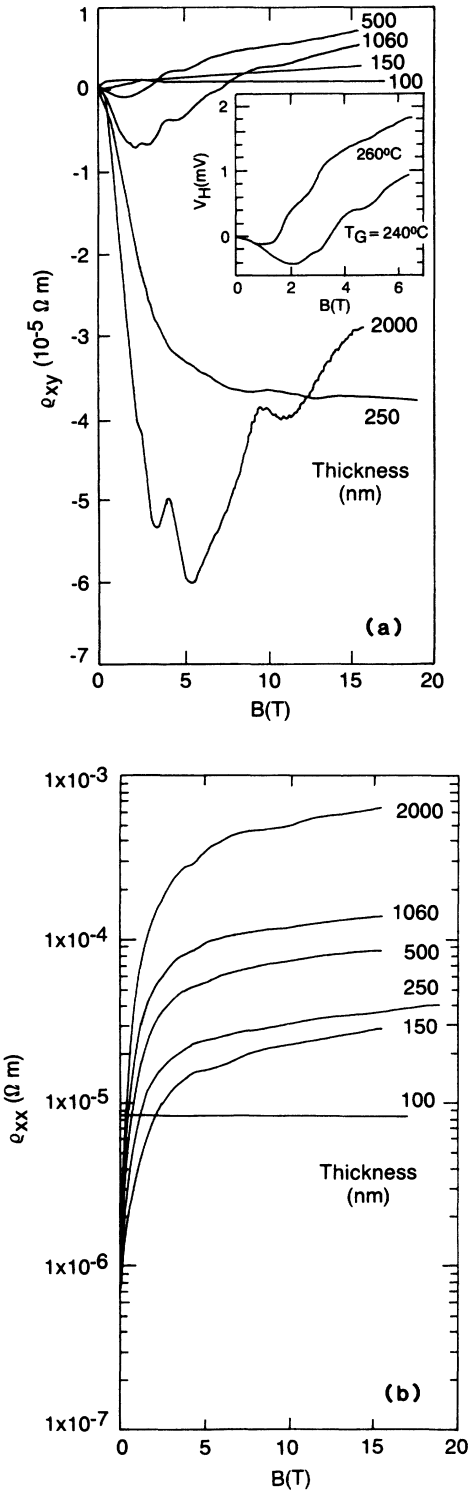

FIG. 6. Hall resistivity ρ_{xy} and magnetoresistivity ρ_{xx} vs magnetic field at 4.2 K for samples of different thickness. The inset shows the Hall voltage up to 7 T at 0.4 K for two 500-nm-thick samples grown at 240 and 260 °C.

The monotonic part of the Hall resistivity is very sensitive to the ratio between electron and hole mobilities; its saturation at high fields is understandable as a result of the linear increase in density. The same holds for the saturation of the magnetoresistance. In pure bulk bismuth, the magnetoresistance is very large at 4.2 K, with $\rho_{xx}(B=5\text{ T})\simeq(4\times10^6)\rho_{xx}(B=0\text{ T})$,[24] because the electron mobility along the ⟨100⟩ axis is limited by phonon scattering to $\simeq10^4$ $m^2V^{-1}s^{-1}$.[16] In our thicker films, the mobility is 100 times smaller and the magnetoresistance is indeed $\sim10^4$ times smaller.

CONCLUSIONS

We have reported on the growth, structure, and galvanomagnetic properties of bismuth films. These films were grown by MBE, and we have shown that the resulting surface morphology is strongly dependent on growth temperature. Samples grown at room temperature have a mottled, polycrystalline texture, whereas as those grown at elevated temperature (near the melting point of bismuth) are smooth and featureless on a 0.1-μm scale. In the latter case the films possess carrier mobilities and densities approaching those of bulk bismuth, and vastly different from those found for films grown by conventional vacuum-evaporation techniques. We also find that the carrier mobility increases with increasing film thickness. Low-temperature–resistivity studies confirm the similarity of these films to single-crystal, rather than polycrystalline, bulk bismuth. Finally, we have observed the first quantum oscillations on a bismuth film and deduce a carrier density from the oscillation period which agrees very well with that determined from the Hall coefficient.

ACKNOWLEDGMENTS

Part of this work was done at the Francis Bitter National Magnet Laboratory, Massachusetts Institute of Technology, supported by the National Science Foundation.

[1]Yu. F. Ogrin, V. N. Lutskii, M. U. Arifova, V. I. Kovalev, V. B. Sandomirskii, and M. I. Elinson, Zh. Eksp. Teor. Fiz. **53**, 1218 (1967) [Sov. Phys.—JETP **26**, 714 (1968)], and references therein.

[2]N. Garcia, Y. H. Kao, and Myron Strongin, Phys. Rev. B **5**, 2029 (1972).

[3]M. Gurvitch, J. Low Temp. Phys. **38**, 777 (1980).

[4]V. N. Lutskii, Pis'ma Zh. Eksp. Teor. Fiz. **2**, 391 (1965) [JETP Lett. **2**, 245 (1965)].

[5]S. Takaoka and K. Murase, J. Phys. Soc. Jpn. **54**, 2250 (1985).

[6]D. Agassi and T. K. Chu, Appl. Phys. Lett. **51**, 2227 (1987).

[7]V. Korenman and H. D. Drew, Phys. Rev. B **35**, 6446 (1987); R. E. Doezema and H. D. Drew, Phys. Rev. Lett. **57**, 762 (1986).

[8]Yu. F. Komnik, E. I. Bukhshtab, A. V. Butenko, and V. V. Andrievsky, Solid State Commun. **44**, 865 (1982).

[9]Yu. F. Komnik, E. I. Bukhshtab, V. V. Andrievskii, and A. V. Butenko. J. Low Temp. Phys. **52**, 315 (1983).

[10]P. H. Woerlee, G. C. Verkade, and A. G. M. Jansen, J. Phys. C **16**, 3011 (1983).

[11]V. D. Das and N. Soundararajan, Phys. Rev. B **35**, 5990 (1987).

[12]Sung-Chul Shin, J. B. Ketterson, and J. E. Hilliard, Phys. Rev. B **30**, 4099 (1984); Sung C. Shin, J. E. Hilliard and J. B. Ketterson, J. Vac. Sci. Technol. A **2**, 296 (1984); Thin Solid Films **111**, 323 (1984).

[13]M. Jalochowski, Phys. Status Solidi A **95**, K5 (1986).

[14]D. L. Partin, J. Electron. Mater. **10**, 313 (1981).

[15]L. Salamanca-Young (private communication).

[16]J-P. Michenaud and J-P. Issi, J. Phys. C **5**, 3061 (1972); R. Hartman, Phys. Rev. **181**, 1070 (1969).

[17]M. S. Dresselhaus, J. Phys. Chem. Solids Suppl. 1, **32**, 3 (1971).

[18]A. A. Lopez, Phys. Rev. **175**, 823 (1968).

[19]D. T. Morelli and J. P. Heremans, General Motors Research Report No. PH-1377, 1987 (unpublished).

[20]C. Uher and W. P. Pratt, Jr., Phys. Rev. Lett. **39**, 491 (1977).

[21]J. M. Ziman, *Electrons and Phonons* (Clarendon, Oxford, 1960).

[22]M. P. Vecchi and M. S. Dresselhaus, Phys. Rev. B **10**, 771 (1974).

[23]J-P. Michenaud, J. Heremans, M. Shayegan, and C. Haumont, Phys. Rev. B **26**, 2552 (1982).

[24]J. H. Mangez, J-P. Issi, and J. Heremans, Phys. Rev. B **14**, 4381 (1976).

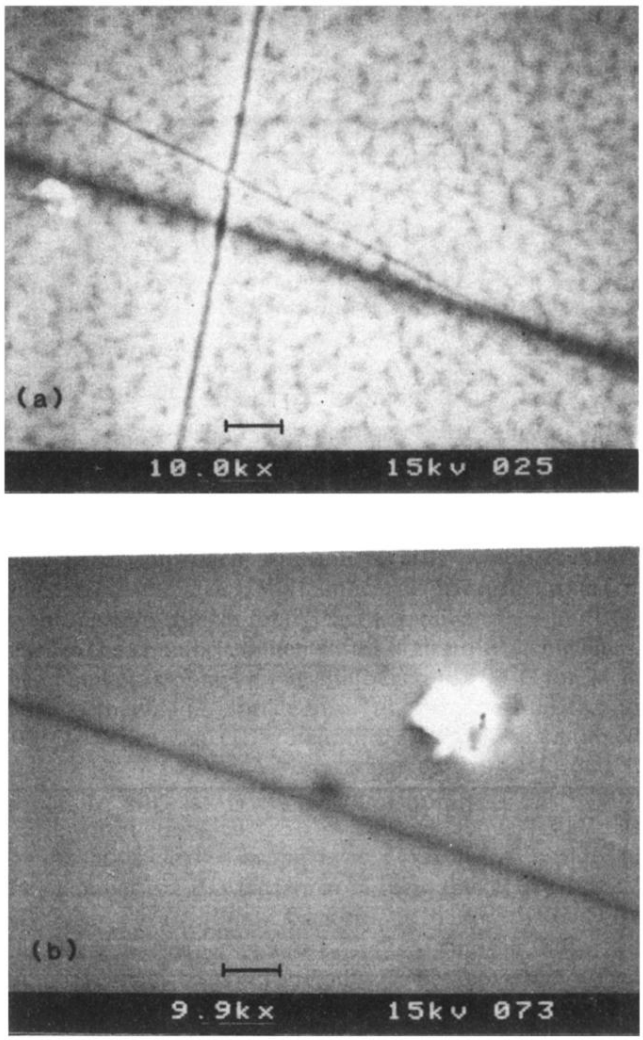

FIG. 1. Scanning-electron micrographs of two bismuth thin films: (a) sample 1, grown at 20 °C; (b) sample 3, grown at 240 °C. Scale is 1 μm.